Chemical and Mechanical Adhesion Mechanisms of Sputter-Deposited Metal on Epoxy Dielectric for High Density Interconnect Printed Circuit Boards

Lara J. Martin, *Member, IEEE,* and C. P. Wong, *Fellow, IEEE*

***Abstract*—Strong chemical reactions between metal and polymer substrates significantly enhance adhesion of the metal to the polymer. This study investigated the adhesion of three types of thin film metals, including Cu, NiCr, and Cr, to a fully epoxy-based polymer. Before depositing these thin film metals, the epoxy surface was treated with either an Ar or O_2 plasma etch. It was found that NiCr and Cr produced higher peel strengths than Cu, but NiCr and Cr did not produce different peel strengths than each other. It was also found that O_2 plasma etch produced significantly higher peel strengths than Ar plasma etch for Cu and Cr, but not for NiCr. An XPS (X-ray photoelectron spectroscopy) study was performed to investigate the reactivities and possible chemical adhesion mechanisms of the metal thin films with the epoxy. It was determined that Cr reacted more strongly than Ni in forming metal oxide at the metal-epoxy interface. Cu was not seen to react strongly in forming oxide with the epoxy. Thermodynamic information supported the relative amounts of oxides found by XPS. Thermodynamic information also suggested that O_2 plasma etch did not produce significantly higher adhesion than Ar plasma etch on the NiCr samples due to the large Ni component of the NiCr thin film. An AFM (atomic force microscopy) study was performed to investigate possible mechanical adhesion mechanisms. Implications of the AFM results were that the main adhesion mechanism for all samples was chemical and that the Cu oxide that was available on the Cu samples was beyond the detection limits of the XPS equipment.**

***Index Terms*—Atomic force microscopy (AFM), build up, chemical adhesion mechanism, design of experiments (DOE), dielectric, epoxy, high density interconnect (HDI), interconnect substrate, mechanical adhesion mechanism, metallize, printed circuit board (PCB), scanning electron microscopy (SEM), sputter, standard Gibbs free energy of formation, statistical tools/methodology, vacuum deposit, x-ray photoelectron spectroscopy (XPS).**

I. INTRODUCTION

WITH trends of increased functionality and reduced size of portable wireless products, increased routing densities for printed circuit boards are resulting. In the case of digital wireless products, high I/O packages (> 144) with pitches of 0.5 to 0.75 mm are typical [1]. High density interconnect, or "build up," printed circuit board technology is becoming a preferred method for constructing circuit boards with such routing density demands. Methods to produce high density printed circuit boards include laser ablating or photoimaging a dielectric material to form interconnect vias that are subsequently metallized by semi-additive electroless copper for layer to layer connections. Typical dielectric materials used in this method are epoxy-based. This method is capable of realizing leading edge printed circuit board design rules of 100 μm vias and 50 μm lines and spaces, producing high routing densities that require reduced layer count when compared to conventional board technology.

Using a material such as a build up epoxy-based dielectric is key to enabling production of highly dense circuit boards, particularly due to space savings realized with the interconnect vias. To produce even more highly dense circuit boards, one option is to further tighten current printed circuit board design rules for line and space widths. If the current line and space design rules are to become more rigorous, an alternative to semi-additive electroless copper must be used to achieve higher resolution. The alternate metallization method that is considered in this study is use of sputter-deposited metal as the metal seed layer. This method presents process design challenges because sputter-deposited metal will have to depend more on chemical adhesion mechanisms than mechanical adhesion mechanisms when compared to electroless copper. Chemical adhesion, based on microscopic-type mechanism, can yield a finer, more uniform adhesion critical for fine lines and spaces than the more macroscopic-type mechanism of mechanical adhesion. If a fundamental understanding of the adhesion mechanisms between the metal and the epoxy-based dielectric can be achieved, a process to produce reliable, next generation high density printed circuit boards can be developed. XPS (X-ray photoelectron spectroscopy) is a powerful tool for detecting metal–polymer reactions, thereby exposing chemical adhesion mechanisms. In a study performed by Davis *et al.*, XPS showed that Cr reacted strongly, Cu reacted mildly, and Ni exhibited little reactivity with a poly(ether imide) substrate [2]. AFM (atomic force microscopy) is an effective tool for investigating surface topographies, thereby establishing evidence of mechanical adhesion mechanisms. This paper will present data on adhesion, quantified as peel strength (running peel strip test), for direct Cu, NiCr, and Cr sputter-deposited on a fully epoxy-based photosensitive dielectric dry film. In addition, this paper will present the effect that surface treatments of Ar plasma etch and O_2 plasma etch had on adhesion of these metal types. Finally, results of XPS and AFM studies that correlate the adhesion mechanism to the quantified peel strength data will be presented.

Manuscript received February 4, 2000; revised March 29, 2001. This work was recommended for publication by Associate Editor P. Garrou upon evaluation of the reviewers' comments.

L. J. Martin is with Motorola, Inc., Plantation, FL 33322 USA (e-mail: lara.martin@motorola.com).

C. P. Wong is with the Packaging Research Center and School of Materials Science and Engineering, Georgia Institute of Technology, Atlanta, GA 30332 USA (e-mail: cp.wong@mse.gatech.edu).

Publisher Item Identifier S 1521-3331(01)07554-7.

1521–3331/01$10.00 ©2001 IEEE

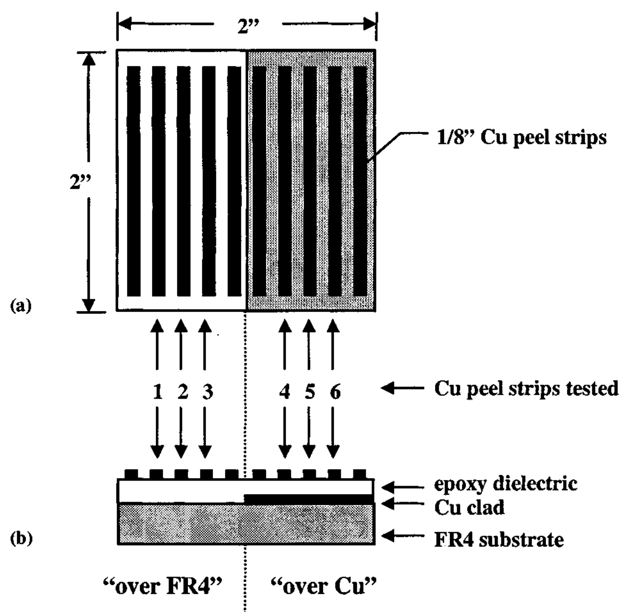

Fig. 1. (a) Top view and (b) cross-sectional view of test coupon design. Half of the coupon area includes the epoxy dielectric directly "over FR4" and the other half includes the epoxy dielectric directly "over Cu". One test coupon was made for each of the six experimental conditions and six peel strips were tested for each test coupon.

TABLE I
AR AND O_2 PLASMA ETCH PARAMETERS

	Ar plasma etch	O_2 plasma etch
base press (mbar)	5E-4	5E-4
ultimate press (mbar)	3E-7	3E-7
power (W)	500	500
gas/rate (sccm)	Ar/150	Ar/10, O_2/100
etch time (min)	0.5	0.5

TABLE II
NICR, CR, AND CU SPUTTER PARAMETERS

	NiCr	Cr	Cu
base press (mbar)	8E-6	8E-6	8E-6
ultimate press (mbar)	3E-7	3E-7	3E-7
power (W)	4,500	4,500	11,250
gas/rate (sccm)	Ar/150	Ar/150	Ar/150
metal thickness (Å)	700 ±100	700 ±100	2100 ±100

TABLE III
PEEL STRENGTH TEST PARAMETERS

peel strip metal thickness	0.028 ±0.010 mm
peel strip width	3.175 mm
peel length	10 ±3 mm
crosshead speed	50.8 mm/min
sampling rate	6 points/sec

II. EXPERIMENTAL

Design of experiments (DOE) methodology was used to quantify peel strength. The measured response for the designed experiment was peel strength. Factors of the DOE included surface treatment and metal type. For this experimental design, the two levels of surface treatment were Ar and O_2 plasma etches. The three levels of metal type were direct Cu, NiCr/Cu, and Cr/Cu. All 6 possible combinations of these factors were measured. For each of the 6 combinations of factors, 6 data points were obtained, totaling 36 data points taken for the entire experiment.

The test coupon design used to obtain peel strength measurements is shown schematically in Fig. 1. To begin processing of the test coupons, print and etch of a copper clad panel of FR4 was performed. Next, a dry film of photosensitive epoxy dielectric was applied, flood exposed, developed, and cured. Then, the panel was routed to singulate the test coupons. Six test coupons, one for each of the 6 combinations of factors, were then surface treated (Ar or O_2 plasma etch) and metallized (Cu, NiCr/Cu, or Cr/Cu) using a Leybold in-line vacuum sputtering system type Z600 with a Polycold trap. The plasma etch and sputter parameters are given in Tables I and II, respectively. Because both the plasma etch and sputtering were done within the Leybold sputtering system, no exposure of the coupons to atmosphere occurred between surface treatment and metallization. For the coupons with Cu metal type, only Cu was sputtered. For the coupons with NiCr/Cu, the coupons were sputtered with NiCr followed by Cu in the same sputter chamber. Likewise, the coupons with Cr/Cu were sputtered with Cr followed by Cu in the same sputter chamber. Sputter parameters for Cu listed in Table II were used in cases that Cu was sputtered directly onto the epoxy dielectric as well as in cases that Cu was sputtered as an overlayer on top of NiCr or Cr. Immediately after pump down of the sputter chamber but prior to metal plasma ignition for sputter, RGA (residual gas analyzer) data was taken. As listed in Table II, the pressure at this time of processing (base pressure) was approximately 8E-6 mbar. By inspection of the RGA data, the main species detected was water. After surface treatment and metallization of the test coupons was complete, the Cu peel strips were built up using semi-additive processing techniques: application and patterning of plating resist, Cu electroplating, resist strip, and sputter metal etch. Wet etches used for the sputtered Cu, NiCr, and Cr are standard industry etches [3].

After processing of the test coupons was complete, the coupons and equipment were prepared for peel strength tests. Metal leads that were the same width as the Cu peel strips (2.175 mm) were soldered onto the Cu peel strips. The strips were then pulled from the epoxy so that running peel measurements could be immediately obtained. The equipment used for the peel test was an Instron model number 5567. The coupon to be tested was rigidly secured in an Instron fixture that maintained a 90° peel angle during the peel test. The peel strength test was then performed. The parameters of the peel strength test are summarized in Table III. A single peel strength measurement was obtained for each peel strip by averaging the running peel load for the peel length of 10 ± 3 mm.

The 36 data points that were obtained from the peel strength test were statistically analyzed in order to quantify peel strength results. The software utilized in the statistical analyzes was JMP [4]. A number of statistical tests were performed including a fit model platform based on least squares and Bayes plot platform based on probability.

TABLE IV
XPS PARAMETERS * SPUTTER RATE REPORTED AS SiO_2 SPUTTER RATE

equipment	PHI Quantum 2000-1
X-ray source	monochromated Al Kα
XPS spot diameter	200 μm
base pressure	1E-8 Torr
pass energy	93 eV
sputter ion current species	Ar
sputter ion current	2 μA
sputter voltage	2 keV
sputter angle	45°
sputter raster size	2 mm X 2 mm
sputter rate *	120 Å/min
sputter intervals	0.5 min
sputter sample position	Zalar rotation

Upon completing the DOE section of the study to quantify peel strength, an analysis using SEM (scanning electron microscopy) and EDS (energy dispersive spectroscopy) was performed to investigate the failure interface during the peel strength test. Both the underside of the Cu peel strip and the corresponding epoxy surface were investigated for the sample with the lowest peel strength and the sample with the highest peel strength. An AMRAY model number 1830I SEM equipped with an EDAX International EDS was used for this analysis. The surfaces were studied at 565× magnification.

With verification of the main failure interface during the peel strength test, an XPS study was performed to investigate chemical adhesion mechanisms. At the same time that the peel strength test coupons were processed, coupons to be studied using XPS were processed. To process the XPS coupons, 6 coupons (taken from the same panel described above) were processed using the same plasma etch and metal sputter parameters listed in Tables I and II, respectively, with one exception. During metal sputter, a conveyor speed increased by a factor of 1.7 was used, which effectively decreased the sputter metal thickness on the XPS coupons by slightly less than half those thicknesses listed in Table II. The coupons were then analyzed by XPS using PHI Quantum 2000-1 equipment. The XPS parameters that were used during the study are listed in Table IV. For these XPS parameters, the resolution of the XPS was an effective FWHM of 1.5 eV measured for the $Cu2p_{3/2}$ peak.

Finally, an AFM study was performed to investigate mechanical adhesion mechanisms. At the same time that the peel strength test coupons were processed, coupons to be studied using AFM were processed. To process the AFM coupons, three coupons were taken from the same panel described above. One of the three coupons was maintained as an untreated surface, or control. Another of these coupons was processed using the Ar plasma etch parameters listed in Table I. The last of the three coupons was processed using the O_2 plasma etch parameters listed in Table I. A Digital Instruments Dimension™ 3100 Series scanning probe microscope was used in tapping mode for this analysis. This AFM was equipped with NanoProbe™ SPM tips type TESP with specified tip radius of 5–10 nm. AFM scans for 500 nm × 500 nm and 300 nm × 300 nm areas were obtained for each of the three coupons. Then, another set of scans were obtained as a replication, totaling 12 scans

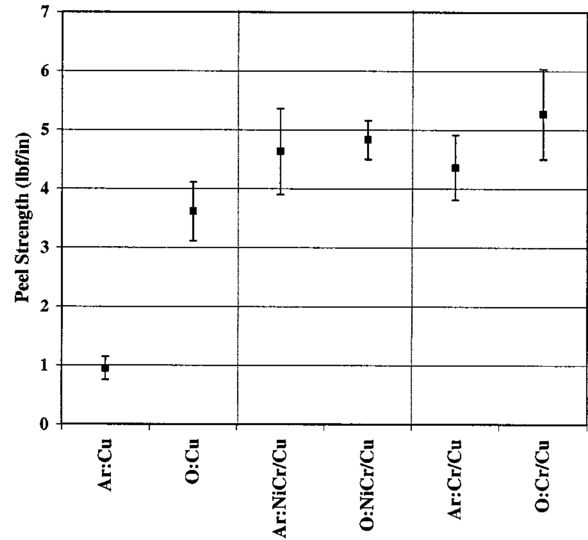

Fig. 2. Average peel strengths and standard deviations. six peel strength measurements were taken for each of the six conditions.

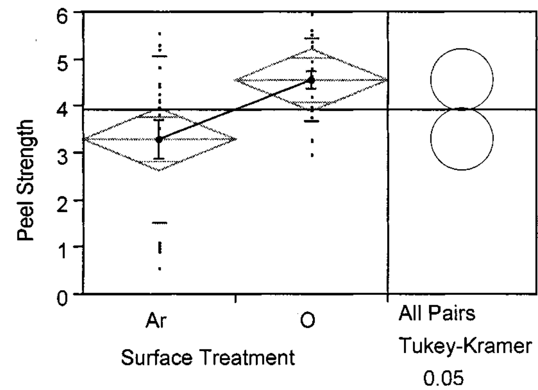

Fig. 3. Statistical analysis of peel strength by surface treatment. Comparison circles to right show surface treatments of Ar and O_2 to be significantly different at the 95% confidence level.

taken in all. The Dimension 3100™ AFM in tapping mode is specified to have nanometer in plane resolution and better than 0.1 nm vertical resolution.

III. RESULTS

A. Measured Adhesion

The graph of the adhesion results is shown in Fig. 2. The six peel strength means and standard deviations shown were each determined from six peel strength measurements. Control samples, for which the thin films were deposited directly onto untreated epoxy surfaces, were found to have no adhesion as the metal peeled from the epoxy surface during sample preparation.

The statistical analyzes that were performed on the peel strength measurements, including those analyzes based on least squares as well as those based on probability, yielded the same results. These results are summarized in Figs. 3 and 4, which show results of the Fit Y by X platform in JMP software. These figures can be interpreted with the following information: group means are represented by bold dots and are shown with error

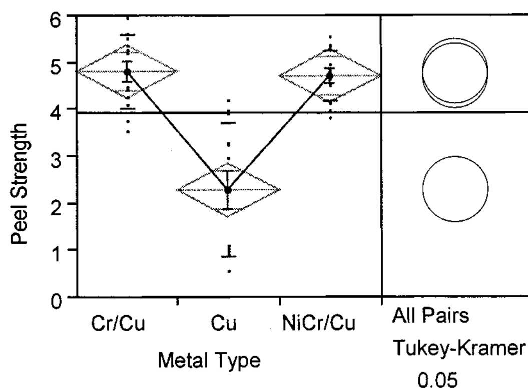

Fig. 4. Statistical analysis of peel strength by metal type. Comparison circles to right show Cu metal type to be significantly different from Cr and NiCr metal type but Cr not significantly different from NiCr at the 95% confidence level.

bars of one standard error; means of the groups are connected; diamond heights are 95% confidence intervals and diamond widths represent group sample sizes; and horizontal lines seen outside of and on diamonds represent one standard deviation.

By inspection of the comparison circles that represent populations determined for the conditions, Fig. 3 shows that, when metal types are taken together, O_2 produced significantly higher peel strengths than Ar plasma etch at the 95% confidence interval. Likewise, Fig. 4 shows that Cr and NiCr produced significantly higher peel strengths than Cu but Cr did not produce significantly higher peel strengths from NiCr. In addition, these figures show that the difference between metal types of Cu versus Cr and NiCr is greater than the difference between surface treatments of Ar and O_2 plasma etches.

To investigate the effect of surface treatment within the metal types, the same statistical tools were applied. Significantly higher peel strength measurements for O_2–treated samples were verified at the 95% confidence interval compared to Ar-treated samples for both Cu and Cr metal types, but failed to be verified for NiCr metal type.

Additional statistical analyzes were done to determine if, for each of the six test coupons, the peel strengths obtained "over FR4" were significantly different from those obtained "over Cu." At the 95% confidence level, the conditions of "over FR4" versus "over Cu" did not produce significantly different peel strength results.

B. *Failure Interface Analysis*

An SEM study was performed to determine the main failure interface during the peel strength tests. At a magnification of 565×, essentially no material was seen on the underside surface of the Cu peel strips for the Ar: Cu coupon, the sample with the lowest peel strength. EDS was used and verified pure Cu. At the same magnification, small areas (< 1 mil) of material were seen on the Cu peel strip underside surface for the O: Cr/Cu coupon, the sample with the highest peel strength. EDS detected the elements C, O, Mg, Ca, Cr, and Cu, indicating the material was the epoxy dielectric with calcium carbonate—magnesium carbonate filler. In effect, the SEM study verified the main failure interface to be metal-epoxy.

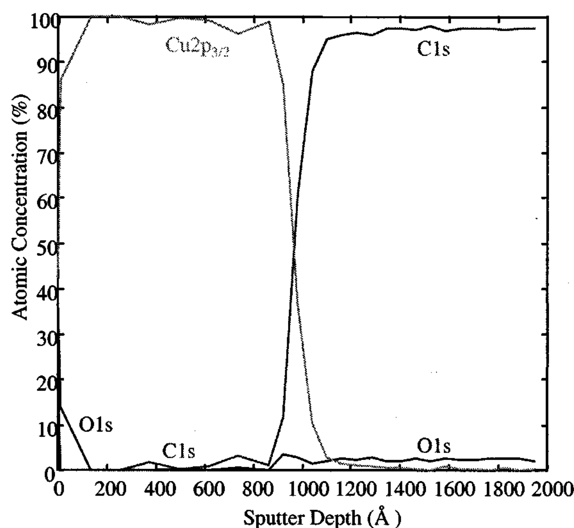

Fig. 5. XPS depth profile of metal-epoxy interface for Ar: Cu sample.

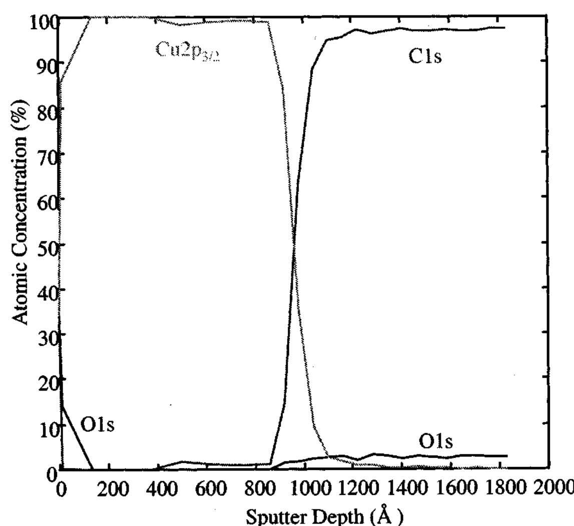

Fig. 6. XPS depth profile of metal-epoxy interface for O: Cu sample.

C. *XPS Analysis*

To understand the peel strength results that were obtained, an XPS study was conducted to investigate the chemical adhesion mechanisms. Because the condition of "over FR4" did not produce significantly different peel strength results compared to "over Cu" per statistical analyzes, the metal-epoxy interfaces "over Cu" was the side of the XPS coupons arbitrarily chosen from which all XPS data was obtained.

The XPS depth profiles for Ar: Cu and O: Cu are shown in Figs. 5 and 6, respectively. The peak atomic concentrations of O for both of these profiles are 4%.

For the Ar: Cu and O: Cu samples, O1s spectra were obtained. The O1s spectrum for O: Cu sample is shown in Fig. 7. The O1s spectrum for Ar: Cu sample is almost identical to that shown in Fig. 7, and, therefore, is not included here. In this O1s spectrum as well as all other spectra presented in this study, the individual lines represent the XPS data taken throughout the metal layer, with the upper-most line taken at the beginning of the profile to the bottom-most line taken at the end of the profile and, therefore, deepest in the interface. By inspection of the lines just

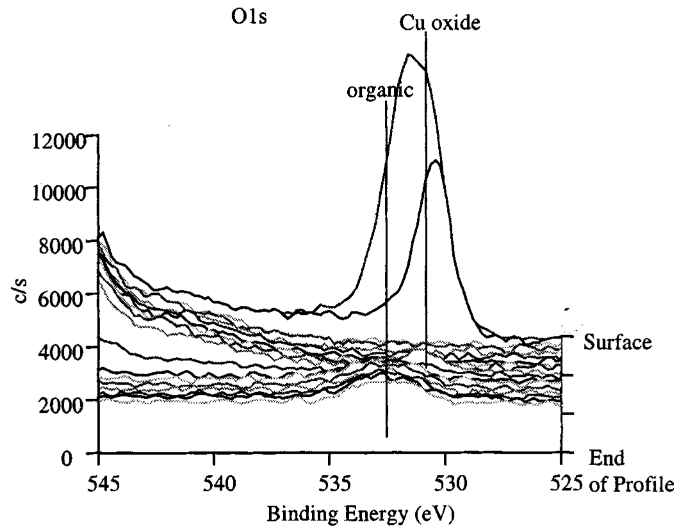

Fig. 7. Ols spectrum for O: Cu sample.

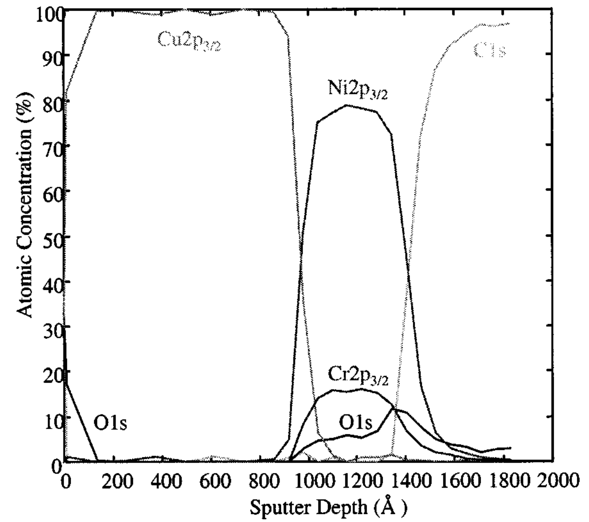

Fig. 9. XPS depth profile of metal-epoxy interface for O: NiCr/Cu sample.

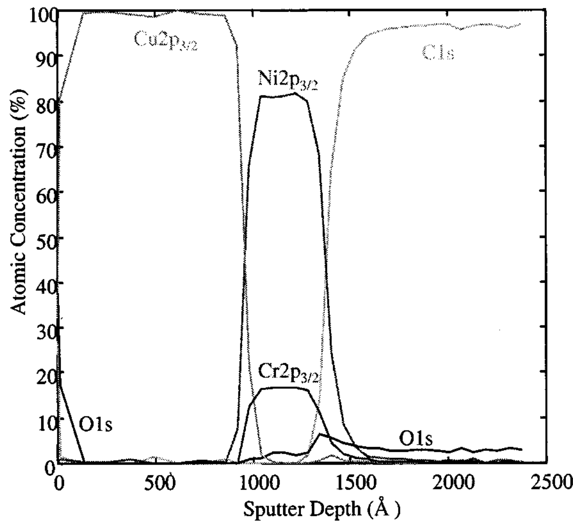

Fig. 8. XPS depth profile of metal-epoxy interface for Ar: NiCr/Cu sample.

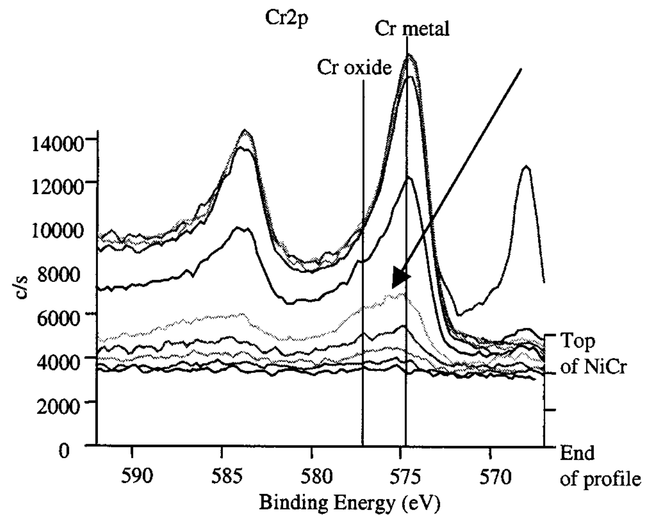

Fig. 10. Cr2p spectrum for Ar: NiCr/Cu sample. Arrow shows peak with Cr metal and Cr oxide character.

below the Cu surface to the organic (epoxy) interface for the Ar: Cu and O: Cu samples, no significant amount of metal oxide is seen.

Finally, for the Ar: Cu and O: Cu samples, $Cu2p_{3/2}$ and Cu Auger spectra were obtained. These spectra were characteristic for Cu metal. $Cu2p_{3/2}$ and Cu Auger spectra characteristic for Cu metal can be referenced in literature [2].

The depth profiles through the metal-epoxy interface for Ar: NiCr/Cu and O: NiCr/Cu samples are shown in Figs. 8 and 9, respectively. The peak atomic concentrations for Ni on these Ar- versus O_2-treated samples are similar at 82% and 79%, respectively. The peak atomic concentrations for Cr are also similar at 17% and 16%, respectively. As validation that these results are reasonable, the atomic concentrations for Ni and Cr found on these samples are close to the 80 wt% Ni/20 wt% Cr composition of the NiCr target that was used for NiCr sputter. In addition, the peak atomic concentrations for O on these Ar- versus O_2-treated samples are significantly different at 6% and 12%, respectively.

For the Ar: NiCr/Cu and O: NiCr/Cu samples, Cr2p spectra were obtained. Because these spectra were similar, only the Cr2p spectrum for the Ar: NiCr/Cu sample is shown here as Fig. 10. The Cr2p spectra for both samples contained peaks having Cr metal and Cr oxide character, indicating presence of both Cr metal and Cr oxide. In Fig. 10, an arrow is drawn to show such a peak.

Further, for the Ar: NiCr/Cu and O: NiCr/Cu samples, Ni2p spectra were obtained. Only the Ni2p spectrum for the Ar: NiCr/Cu sample is shown here as Fig. 11. Upon inspection of the Ni2p peaks deepest in the NiCr, spectra for both samples showed peaks having Ni metal and Ni oxide character, indicating presence of both Ni metal and Ni oxide. As further evidence that NiO was detected, shake up peaks for NiO was seen in the spectra for both samples. An arrow is drawn on Fig. 11 to identify the NiO shake up peaks.

Finally, for the Ar: NiCr/Cu and O: NiCr/Cu samples, O1s spectra were obtained. Only the O1s spectrum for the O: NiCr/Cu sample is shown here as Fig. 12. Spectra for both

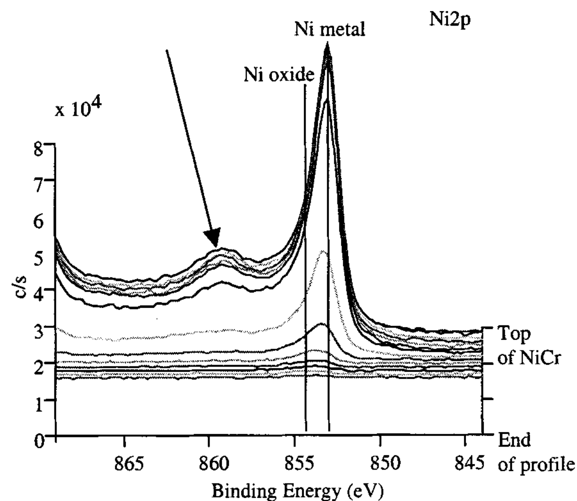

Fig. 11. Ni2p spectrum for Ar: NiCr/Cu sample. Arrow points to NiO shake-up peaks.

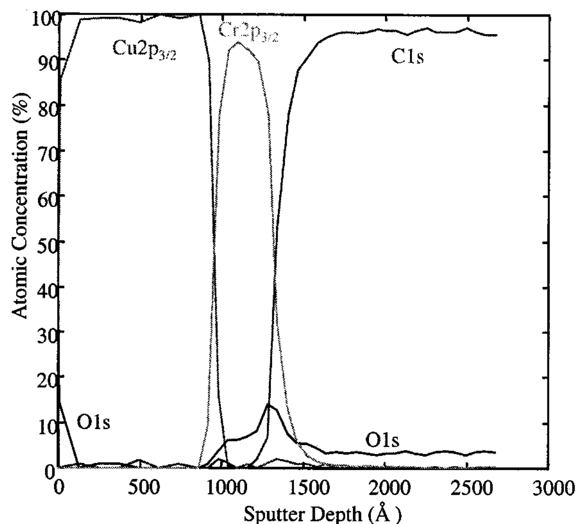

Fig. 13. XPS depth profile of metal-epoxy interface for Ar: Cr/Cu sample.

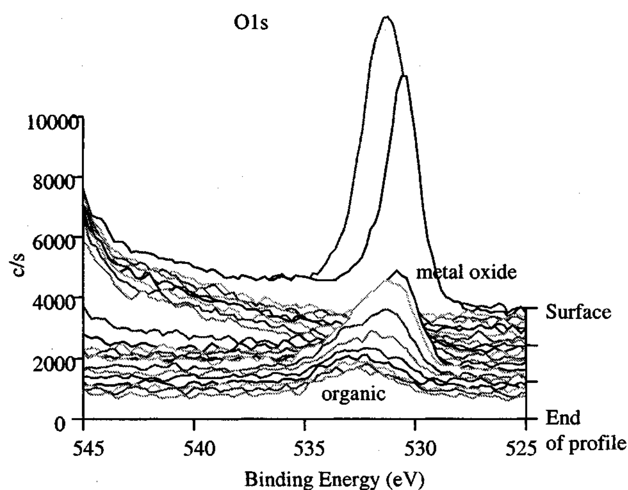

Fig. 12. O1s spectrum for O: NiCr/Cu sample.

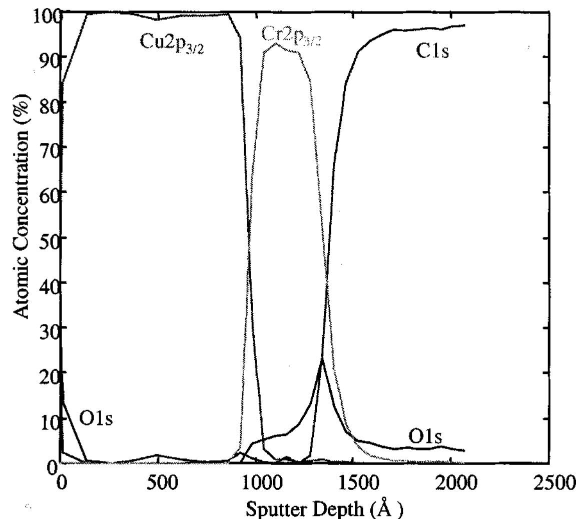

Fig. 14. XPS depth profile of metal-epoxy interface for O: Cr/Cu sample.

samples indicate presence of metal oxide. Because evidence of oxides was determined on the Ni2p and Cr2p spectra for both the Ar: NiCr/Cu and O: NiCr/Cu samples, the metal oxides seen on these O1s spectra are assumed to be both Cr and Ni oxides. Comparing these two spectra, the peaks deepest in the NiCr show a significant increase of metal oxide for the O_2-treated sample.

The depth profiles for the Ar: Cr/Cu and O: Cr/Cu samples are included as Figs. 13 and 14, respectively. The peak concentrations for Cr on the Ar- and O_2-treated samples are both 94%. The peak atomic concentrations for O on these Ar- versus O_2-treated samples are significantly different at 14% and 24%, respectively.

Cr2p spectra were obtained for the Ar: Cr/Cu and O: Cr/Cu samples. Because these spectra were similar, only the Cr2p spectrum for the Ar: Cr/Cu sample is shown here as Fig. 15. Like the Cr2p spectra for the Ar: NiCr/Cu and O: NiCr/Cu samples, the Cr2p spectra for the Ar: Cr/Cu and O: Cr/Cu samples contained peaks having Cr metal and Cr oxide character. In Fig. 15, an arrow is drawn to show such a peak.

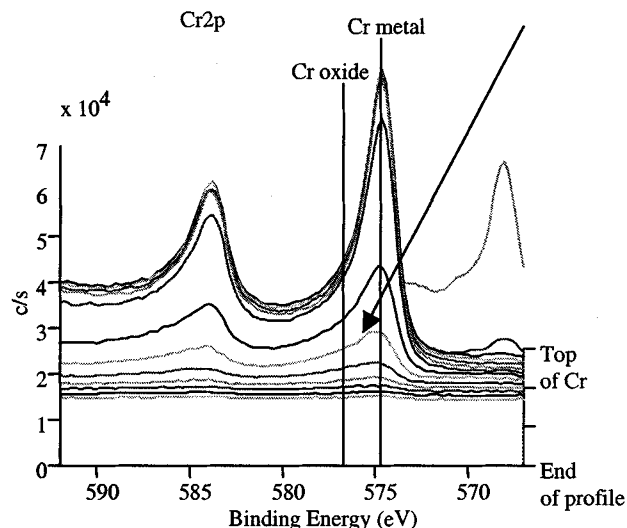

Fig. 15. Cr2p spectrum for Ar: Cr/Cu sample. Arrow shows peak with Cr metal and Cr oxide character.

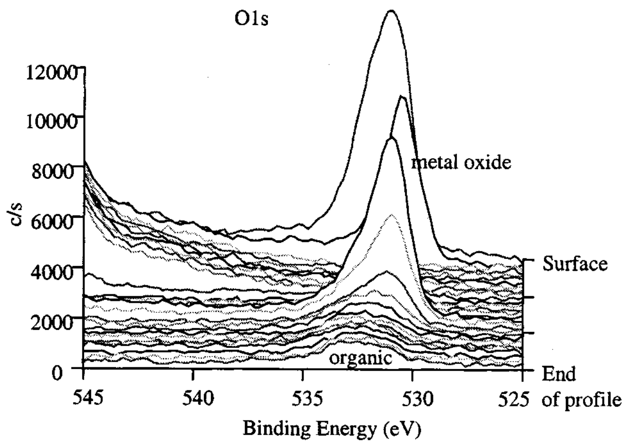

Fig. 16. O1s spectra for O: Cr/Cu sample.

For the Ar: Cr/Cu and O: Cr/Cu samples, O1s spectra were obtained. Only the O1s spectrum for the O: Cr/Cu sample is shown here as Fig. 16. Spectra for both samples indicate presence of metal oxide, or, more specifically, Cr oxide. Comparing these spectra, a significant increase in Cr oxide is seen on the O_2-treated sample.

For all six of the XPS coupons, C1s spectra were obtained as they were utilized to generate all six of the depth profiles. These C1s scans are not shown here because they all are almost identical, with peaks showing expected C–H and C–O bonds from the epoxy.

D. AFM Analysis

An AFM study was performed to determine if the Ar or O_2 plasma etch modified the epoxy dielectric surface and contributed to a mechanical adhesion mechanism. Typical AFM images that were obtained for 500 nm × 500 nm and 300 nm × 300 nm scan areas are shown in Figs. 17 and 18, respectively. Upon inspection of all AFM images, no differences could be verified visually for the untreated, Ar plasma etched, and O_2 plasma etched conditions.

Because no effect of surface treatment could be detected visually, calculations including R_a (average roughness) and S.A. (surface area) were performed on the 12 scans using AFM software. No correlation of R_a to surface treatment was found. However, a correlation of S.A. to surface treatment was determined. Data including the Z range, S.A., and % Increase Over Flat Area are shown for the 500 nm × 500 nm and 300 nm × 300 nm areas in Tables V and VI, respectively. The Z range data is necessary to confirm that no large pits or bulges occurred within the scan area, which would yield incomparable S.A. data. The % Increase Over Flat Area data was calculated as an index to further quantify surface area and to easily compare differences in S.A. data. Upon inspection of the data for both scan sizes, a trend of increasing surface area was recognized from the control to the Ar-treated epoxy to the O_2-treated epoxy. Although this trend was recognized, none of the % Increase Over Flat Area were accepted to be large enough to contribute to differences in a mechanical adhesion mechanism as a main adhesion mechanism.

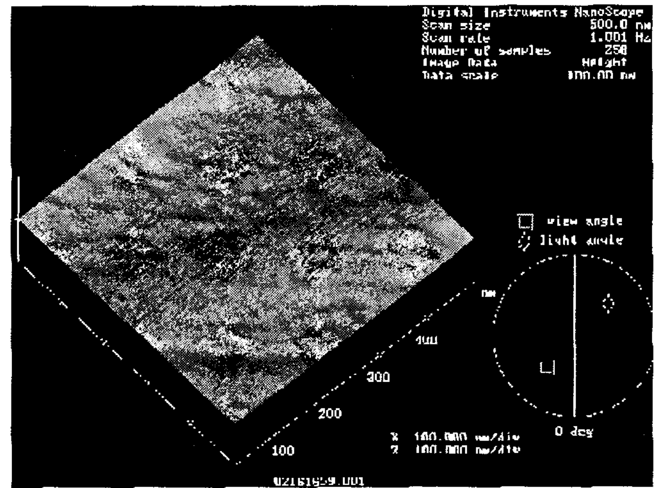

Fig. 17. AFM image of untreated epoxy surface at 500 nm × 500 nm scan size.

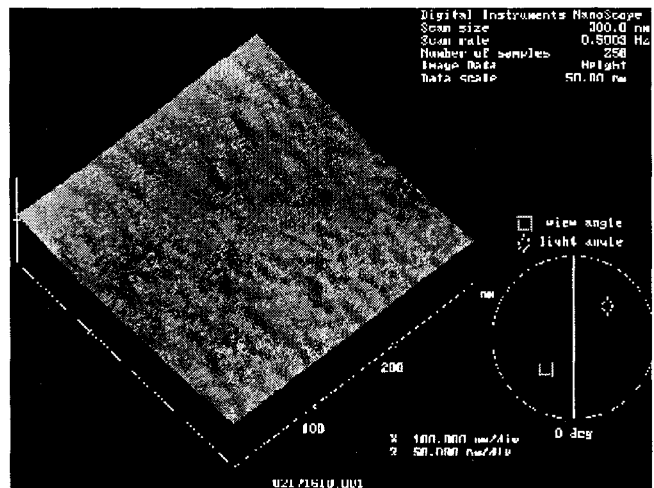

Fig. 18. AFM image of Ar-treated epoxy surface at 300 nm × 300 nm scan size.

TABLE V
SUMMARY OF SURFACE AREAS AS DETERMINED BY AFM FOR 500 nm × 500 nm SCAN AREAS OF UNMETALLIZED EPOXY SURFACES

Surface Treatment	Z Range (nm)	S.A. (nm^2)	% Increase over Flat Area
untreated	8.1	251,524	0.6 %
(control)	6.6	251,431	0.6 %
Ar plasma	13.5	251,607	0.6 %
etch	7.7	251,927	0.8 %
O_2 plasma	12.8	254,268	1.7 %
etch	9.0	257,382	3.0 %

IV. DISCUSSION

A. XPS Implications

The XPS study explained only some of the differences in peel strength data. For direct Cu metal type, XPS analyzes did not give evidence that the difference in peel strengths on the Ar- versus O_2-treated samples could be attributed to a difference in a chemical adhesion mechanism. This evidence was particularly

TABLE VI
SUMMARY OF SURFACE AREAS AS DETERMINED BY AFM FOR 300 nm × 300 nm SCAN AREAS OF UNMETALLIZED EPOXY SURFACES

Surface Treatment	Z Range (nm)	S.A. (nm^2)	% Increase over Flat Area
untreated	8.7	91,063	1.2 %
(control)	10.2	91,298	1.4 %
Ar plasma	9.7	91,475	1.6 %
etch	11.7	91,512	1.7 %
O_2 plasma	10.8	93,133	3.5 %
etch	12.8	92,599	2.9 %

noted as lacking in the O1s spectra for the direct Cu samples. In contrast, the XPS study did give evidence that the significantly higher peel strengths obtained for the O_2- versus Ar-treated samples within the metal type of Cr could be attributed to differences in a chemical adhesion mechanism. Specifically, it was seen by inspection of the O1s spectra for the Cr samples that O_2 plasma etch produced an increased amount of metal oxide at the metal-epoxy interface compared to the Ar plasma etch. The XPS study gave some insight to the NiCr samples. Inspection of the O1s spectra for the NiCr samples showed that O_2 plasma etch produced an increased amount of metal oxide at the metal-epoxy interface compared to the Ar plasma etch. Whereas the increased metal oxides from Ar to O_2 plasma etch resulted in significantly higher measured adhesion for Cr, the increased metal oxides from Ar to O_2 plasma etch did not result in a verifiable significantly higher measured adhesion for NiCr. In addition, the XPS study showed evidence of Cr to be more reactive with the epoxy surface than Ni because of the higher concentration of metal oxide on the Cr sample compared to the NiCr sample. With consideration to all XPS spectra that were investigated, the result of higher metal oxide concentration can be seen in the increased peak atomic concentrations of O for the Cr samples (14% and 24%) versus the NiCr samples (6% and 12%) on the XPS depth profiles.

Thermodynamic data for Cu, NiCr, and Cr does lend support to the XPS results discussed here. The favorability of a metal to form its oxide or for a metal oxide to be oxidized to a higher oxidation state may be quantified by the thermodynamic property of Standard Gibbs Free Energy of Formation. This thermodynamic property is plotted as a function of temperature and shown in Fig. 19 for Cu, Cu_2O, Ni, and Cr. The plot shows that Cr_2O_3 readily forms from Cr as this oxidation reaction has a significantly lower Standard Gibbs Free Energy of Formation than all the other oxidation reactions plotted. Compared to Cr_2O_3, formation of NiO is much less favorable. Formation of Cu_2O is slightly less favorable than the formation of NiO. Also described by the plot, the oxidation of Cu_2O to its higher oxidation state of CuO is the least favorable as this oxidation reaction has the highest Gibbs Free Energy compared to all the oxidation reactions plotted.

Two important aspects of the metal oxides considered in this study may be obtained from this thermodynamic information. First, the more desirable for a metal to form oxide, the more readily the metal may react with the epoxy (an O-rich polymer). Second, the less desirable for a metal to form oxide, the more

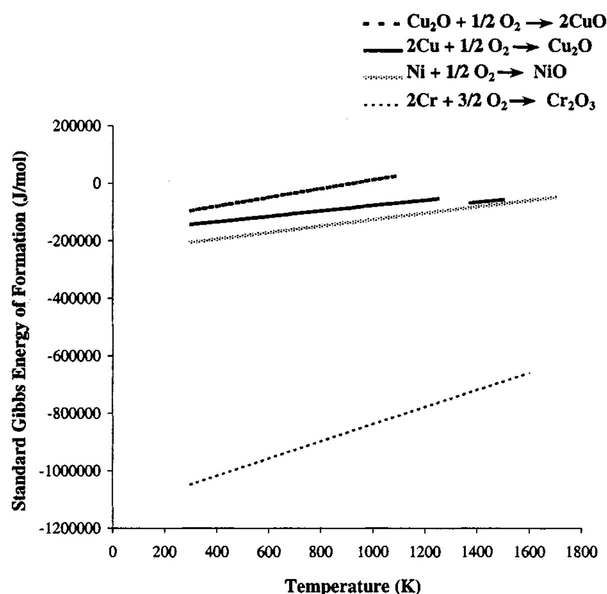

Fig. 19. Standard Gibbs energy of formation for CuO, Cu_2O, NiO, and Cr_2O_3 [5].

easily the metal oxide can be decomposed by a reducing substance, such as the Ar ion sputter used to obtain depth profiles in XPS analyzes. The reduction of metal oxides by Ar ion sputter for spectroscopic depth profiling analyzes has been documented and can be referenced in literature [6], [7]. The thermodynamic information supports why the XPS study, particularly on the O1s spectra, showed the total amount of oxide to be most abundant on the Cr samples followed closely by the total amount of oxides on the NiCr samples and why little to no oxide was detected on the direct Cu samples. Thermodynamic information may also give insight as to why increased metal oxides from Ar to O_2 plasma etch did not result in a verifiable significantly higher measured adhesion for NiCr. The thermodynamic data shows that the affinity for Ni to bond with O is more similar to Cu than Cr, suggesting that the bond strength of Ni and O is more similar to Cu and O than to Cr and O. For the NiCr samples, it is suggested that the main contributor to measured adhesion was the Cr component of the NiCr source (80 wt% Ni/20 wt% Cr) because the strength of the oxide bonds of Cr was greater than that of Ni. Even with the increase of Ni and Cr oxide formation due to the O_2 plasma etch, the net effect of increased Ni oxide was not significant in the adhesion measurements as it was essentially masked by the relatively stronger, more concentrated effect of the Cr oxide.

B. AFM Implications

From the AFM study, AFM images were obtained that showed no visually discernible differences among the untreated, Ar plasma etched, and O_2 plasma etched epoxy dielectric. Moreover, no correlation of R_a to surface treatment was determined. However, a correlation of surface area to surface treatment was identified, specifically, a trend of increasing surface area on the epoxy dielectric from the untreated to the Ar-treated to the O_2-treated surface. Although this correlation was recognized, none of the % Increase Over Flat Area were

accepted to be large enough to contribute to differences in a mechanical adhesion mechanism as a main adhesion mechanism. The first implication of these AFM results was that, for all conditions studied, the main adhesion mechanism attributed to the differences in peel strength measurements was the chemical adhesion mechanism of metal oxidation. The second implication, as taken from the first, was that Cu oxide was available on the Ar: Cu and O: Cu samples but was beyond the detection limits of the XPS equipment.

V. Conclusions

Statistical methodologies were used to determine that NiCr and Cr produced higher peel strengths than direct Cu and that O_2 plasma etch produced higher peel strengths than Ar plasma etch for Cu and Cr metal types, but not for NiCr metal type. Within the Cr samples, the increased peel strength from Ar- to O_2-treated samples could be attributed to a difference in a chemical adhesion mechanism. XPS showed the chemical adhesion mechanism to be the reaction between Cr and the epoxy to form oxide. Within the NiCr samples, XPS showed an increase in oxide formation from Ar- to O_2-treated samples, but this effect did not lead to a significant increase in peel strength. Within the Cu samples, XPS showed no oxide for either the Ar- or O_2-treated samples. Thermodynamic information in the form of the Standard Gibbs Energy of Formation for the metal oxides supported the relative amounts of the different oxides detected by XPS. The thermodynamic information also suggested that the O_2 plasma etch did not significantly enhance adhesion for the NiCr samples due to the large Ni component of the NiCr thin film composition. An implication of the AFM results was that the main adhesion mechanism for all samples was the chemical adhesion mechanism of metal oxidation. To explain the difference in peel strength of the O_2- versus Ar-treated Cu samples, another implication of the AFM results was that the Cu oxide that formed on the Cu samples was beyond the detection limit of the XPS.

Acknowledgment

The authors wish to thank T. Swirbel for his vision, generosity, and guidance, K. Arledge and F. So for their direction, A. Hogrefe and L. Davis for their XPS expertise, J. Frei for many discussions on statistics, and J. Barreto, who is responsible for making this work possible.

References

[1] T. J. Swirbel, "Substrate requirements for effective integration of chip scale packages and multichip modules," *Int. J. Microcirc. Electron. Packag.*, vol. 22, no. 3, pp. 248–253, 1999.

[2] J. L. Davis *et al.*, "Spectroscopic studies of the chemical properties of thin metal films on Poly(ether imide)," *Thin Solid Films*, vol. 220, pp. 217–221, 1992.

[3] *Sputtering Targets and Evaporation Sources*, Materials Research Corporation, New York, 1985, pp. 7-4–7-7.

[4] *JMP Version 3.2.6*, SAS Institute, Inc, Cary, NC.

[5] D. R. Lide, Ed., *CRC Handbook of Chemistry and Physics*, 77th ed. Boca Raton, FL: CRC, 1996–1997, pp. 5-89–5-92.

[6] D. F. Mitchell *et al.*, "Sputter reduction of oxides by ion bombardment during Auger depth profile analysis," *Surf. Interface Anal.*, vol. 15, no. 8, pp. 487–497, 1990.

[7] H. J. Mathieu *et al.*, "Depth profile analysis of thin oxide films by Auger electron spectroscopy," *IEEE Trans. Nucl. Sci.*, vol. 3, pp. 2023–2026, Sept. 1977.

Lara J. Martin (M'98) received the B.S. degree in chemical engineering and the M.S. degree in materials science and engineering, both from the Georgia Institute of Technology, Atlanta.

She is a Senior Engineer in Advanced Product Technology Center, Motorola, Inc., Plantation, FL. Her background is in the areas of printed circuit board and thin film process development. She holds several U.S. patents and an international patent and is a recognized Motorola Six Sigma Black Belt for her knowledge and extensive application of statistical methodologies.

C. P. Wong (SM'87–F'92) received the B.S. degree in chemistry from Purdue University, West Lafayette, IN, and the Ph.D. degree in organic/inorganic chemistry from Pennsylvania State University, University Park.

After his doctoral study, he was awarded two years as a Postdoctoral Scholar at Stanford University, Stanford, CA. He joined AT&T Bell Laboratories, in 1977 as Member of Technical Staff. he was elected an AT&T Bell Laboratories Fellow in 1992. He is a Regents Professor with the School of Materials Science and Engineering and a Research Director at the NSF-funded Packaging Research Center, Georgia Institute of Technology, Atlanta. He holds over 45 U.S. patents, numerous international patents, and over 300 technical papers in the related area. His research interests lie in the fields of polymeric materials, high Tc ceramics, materials reaction mechanism, IC encapsulation, in particular, hermetic equivalent plastic packaging, electronic manufacturing packaging processes, interfacial adhesions, PWB, SMT assembly, and components reliability.

Dr. Wong received the AT&T Bell Laboratories Distinguished Technical Staff Award in 1987, the AT&T Bell Labs Fellow Award in 1992, the IEEE Components, Packaging and Manufacturing Technology (CPMT) Society Outstanding and Best Paper Awards in 1990, 1991, 1994, 1996, and 1998, the IEEE Technical Activities Board Distinguished Award in 1994, the 1995 IEEE CPMT Society's Outstanding Sustained Technical Contribution Award, the 1999 Georgia Tech's Outstanding Faculty Research Program Development Award, the 1999 NSF-Packaging Research Center Faculty of the Year Award, the Georgia Tech Sigma Xi Faculty Best Research Paper Award in 2000, the University Press (London, UK) Award of Excellence in 2000 and the IEEE Third Millennium Medal in 2000. He is a Fellow of AIC and AT&T Bell Labs. He served as the Technical Vice President (1990 and 1991) and the President (1992 and 1993) of the IEEE-CPMT Society and was elected a member of the National Academy of Engineering in 2000.